Bitlis Eren Üniversitesi Fen Bilimleri Dergisi
BİTLİS EREN UNIVERSITY JOURNAL OF SCIENCE
ISSN: 2147-3129/e-ISSN: 2147-3188
VOLUME: 13 NO: 3 PAGE: 723-730 YEAR: 2024
DOI:10.17798/bitlisfen.1479292

Phenylsulfonylpiperazines as α-Glucosidase Enzyme Inhibitors: Design, Synthesis, DFT Calculations, Docking and ADME Studies

Kerem BURAN [1*], Yiğit İNAN [2], Gülşah Selin AKYÜZ [3], Celile DERVİŞOĞLU[5] ÖZDEMİR [4,5], Fatih KOCABAŞ [6]

[1] *Department of Pharmaceutical Chemistry, Hamidiye Faculty of Pharmacy, University of Health Sciences, 34668 İstanbul, Türkiye.*
[2] *Department of Pharmacognosy, Hamidiye Faculty of Pharmacy, University of Health Sciences, 34668, İstanbul, Türkiye.*
[3] *Department of Pharmacognosy, School of Pharmacy, Bahçeşehir University, İstanbul, Türkiye.*
[4] *Department of Chemistry, Institute of Science, Marmara University, 34720 Goztepe, İstanbul, Türkiye.*
[5] *Department of Analytical Chemistry, Faculty of Pharmacy, Istanbul Health and Technology University, 34445, Beyoglu, İstanbul, Türkiye.*
[6] *Department of Genetics and Bioengineering, Faculty of Engineering, Yeditepe University, Istanbul, Türkiye.*

(ORCID: 0000-0002-7783-7533) (ORCID: 0000-0002-3253-0124) (ORCID: 0000-0002-8455-8970) (ORCID: 0000-0001-8603-3820) (ORCID: 0000-0001-8096-6056)

Keywords: Diabetes mellitus, α-Glucosidase, Sulfonamide, Piperazine, DFT calculations.

Abstract

Diabetes mellitus (DM) is one of the most common diseases affecting people all over the world. An important treatment for DM is the inhibition of the α-glucosidase enzyme. A wide range of biological activities of piperazine and sulfonamide moieties are known. In this study, five phenylsulfonyl piperazine derivatives were synthesized. Their inhibitory capacities were evaluated. The analogues (**1**-**5**) showed a good degree of inhibition of α-glucosidase enzyme. Compound **1** has the highest inhibition potential for the α-glucosidase enzyme. Its inhibition percentages (83.52±0.41) were higher than the reference molecule quercetin (81.41±0.02). *In silico* molecular docking studies were performed for the most potent compound **1** for α-glucosidase enzyme to determine possible protein-ligand interactions. Furthermore, a DFT study was carried out for the evaluation of the quantum mechanical and electronic properties. Finally, ADME profiles of the compounds were theoretically analyzed.

1. Introduction

Diabetes mellitus (DM) is one of the most common metabolic diseases in the world. DM is characterized by low insulin levels and high blood glucose levels. In the case of damage to pancreatic cells, abnormalities in insulin secretion occur and this phenomenon is called hyperglycemia. Hyperglycemia causes significant health problems in vital organs such as, blood vessels, kidneys, eyes, brain, and heart [1]. DM is mainly categorized into two subtypes which are Type 1 (T1DM) and Type 2 (T2DM) DM. The low level of insulin is the major reason for these subtypes of DM [2]. There are some factors that cause high levels of glucose in the human body such as high activity of α-amylase and α-glucosidase enzymes. α-amylase (E.C. 3.2.1.) is an enzyme that breaks down carbohydrates like starch to monosaccharides in the human body. Further degradation is continued to glucose by the α-glucosidase enzymes. Because of their important role in carbohydrate digestion process, inhibition of these enzymes can decrease degradation of carbohydrate, postpone glucose consumption, and decrease blood glucose level [3]. Therefore,

*Corresponding author: kerem.buran@sbu.edu.tr
Received: 07.05.2024, Accepted: 09.09.2024

inhibition of these enzymes has become an important strategy to treat T2DM. Acarbose, Voglibose and Miglitol have been discovered and used as drug for treatment of T2DM. Although there are some side-effects such as flatulence and diarrhea. Acarbose is used for treatment of T2DM worldwide [4].

The piperazine heterocycle is one of the most important moieties for drug molecules. It can be used as a main scaffold or be moiety for molecular hybridization. Vitaku *et al*. investigated that drugs which were approved by U.S. Food and Drug Administration (FDA) [5] . According to this study, piperazine heterocycle is the third most common nitrogen heterocycles which participated in the FDA approved drugs. Additionally, piperazine derivatives have different pharmacological activities such as anticancer [6], anticonvulsant [7], antianginal [8], anti-inflammatory [9], carbonic anhydrase enzyme inhibitor [10]. Another important functional structure with various biological activities is sulfonyl structures. The sulfonyl group either contributes to the biological activities of the molecules to which they are attached, or the derivatives have biological activities. These biological activities are anti-inflammatory activity [11], anticancer [12] and antidiabetic [13].

In this study, it was investigated that inhibition potential of sulfonyl-piperazine molecules against α-glucosidase enzyme. Docking studies and Density Functional Theory (DFT) calculations were done for correlating biological activity and molecular properties. Additionally, for investigation of ADME properties of compounds bioavailability radar charts were calculated. While Xiao *et al*. [14] synthesized two phenylsulfonyl piperazine derivatives without probing their biological activities, and Abbasi *et al*. [15] synthesized and reviewed similar compounds without focusing on their α-glucosidase inhibition, this study bridges these gaps. Emphasis is placed on compound 2, which earlier reports have not evaluated for α-glucosidase enzyme activity or through Density Functional Theory (DFT) calculations. Our comprehensive approach includes docking studies and DFT calculations to correlate biological activities with molecular properties, as well as ADME analysis via bioavailability radar charts to predict pharmacokinetic behavior. This research could pave the way for improved treatments of T2DM with optimized therapeutic profiles and reduced side effects.

2. Material and Method

2.1. Chemicals

2.1.1. Materials and reagents

All the chemicals were purchased from Fluka Chemie AG Buchs and Sigma Aldrich and used without further purification. Reactions were monitored by thin-layer chromatography (TLC) on silica gel 60 F254 aluminium sheets. The mobile phase was ethyl acetate: *n*-Hexane (1:1), and detection was made using UV light. ^{1}H NMR and ^{13}C NMR spectra were registered in $CDCl_3$ on Agilent 400/54 (400 MHz) NMR. The mass spectra were obtained on Agilent 6530 Accurate Mass Q-TOF LC/MS.

2.1.2. General procedure for the synthesis of compounds 1-5

Triethylamine (3.0 eq) was added slowly to a solution of piperazine derivatives (1.0 eq) CH_2Cl_2 at 0 °C, then to this was added benzene sulfonyl chloride (1.0 eq) and stirred for 2 hours. The completion of the reaction was checked with TLC (*n*-hexane and ethyl acetate (1:3)). After the reaction was finished, the solution was quenched with water and extracted with CH_2Cl_2. The combined organic layer was dried over anhydrous Na_2SO_4 and evaporated to give compounds **1-5** [13].

1-Ethyl-4-(phenylsulfonyl)piperazine (1)

Yield: 90%, grey solid. ^{1}H NMR (400 MHz, $CDCl_3$) δ 7.72 (d, *J* = 7.4 Hz, 2H), 7.52 (dt, *J* = 14.1, 6.8 Hz, 3H), 3.01 (s, 4H), 2.48 (s, 4H), 2.36 (dd, *J* = 14.2, 7.1 Hz, 2H), 0.99 (t, *J* = 7.1 Hz, 3H); ^{13}C NMR (400 MHz, $CDCl_3$) δ 135.1, 132.7, 128.9, 127.8, 76.7, 51.8, 46.0, 11.8; HRMS (ESI) calcd for $C_{12}H_{18}N_2O_2S$ $[M + H]^+$ m/z: 255.1189, found 255.1161.

1-Phenyl-4-(phenylsulfonyl)piperazine (2)

Yield: 78%, white solid. ^{1}H NMR (400 MHz, $CDCl_3$) δ 7.77 (d, *J* = 7.2 Hz, 2H), 7.57 (dt, *J* = 25.8, 7.2 Hz, 3H), 7.27 – 7.19 (m, 2H), 6.84 (d, *J* = 7.9 Hz, 3H), 3.18 (dd, *J* = 21.2, 4.4 Hz, 8H). ^{13}C NMR (400 MHz, $CDCl_3$) δ 150.5, 135.2, 133.0, 129.1, 127.7, 125.9, 120.7, 116.8, 49.1, 46.0. HRMS (ESI) calcd for $C_{16}H_{18}N_2O_2S$ $[M+H]^+$ m/z: 302.1089, found 302.8967.

1-(3-Fluorophenyl)-4-(phenylsulfonyl)piperazine (3)

Yield: 78%, light pink. ^{1}H NMR (400 MHz, $CDCl_3$) δ 7.78 (d, *J* = 7.4 Hz, 2H), 7.58 (dt, *J* = 28.2, 7.3 Hz, 3H), 7.42 – 7.29 (m, 1H), 6.85 – 6.57 (m, 3H), 3.28 (d, *J* = 12.4 Hz, 8H), 1.34 (t, *J* = 7.3 Hz, 1H); ^{13}C NMR (400 MHz, $CDCl_3$) δ 164.7, 162.3, 135.3, 133.2, 130.7, 129.2, 128.2, 127.7, 125.8, 49.6, 46.1,

45.3; HRMS (ESI) calcd for $C_{16}H_{17}N_2O_2FN_2S$ $[M+H]^+$ m/z: 321.0995 found 321.0329.

1-(4-Methoxyphenyl)-4-(phenylsulfonyl) piperazine (4)

Yield: 63%, light pink solid. ^{1}H NMR (400 MHz, $CDCl_3$) δ 7.79 (d, *J* = 7.2 Hz, 2H), 7.58 (m, 3H), 6.84 (m, 4H), 3.74 (s, 2H), 3.17 (d, *J* = 25.3 Hz, 8H); ^{13}C NMR (400 MHz, $CDCl_3$) δ 135.3, 133.0, 129.1, 127.7, 125.8, 119.3, 114.5, 55.5, 50.8, 46.0; HRMS (ESI) calcd for $C_{16}H_{17}FN_2O_2S$ $[M+H]^+$ m/z: 332.1195 found 332.0596.

4-(Phenylsulfonyl)piperazine-1-carbaldehyde (5)

Yield: 84%, white solid. ^{1}H NMR (400 MHz, $CDCl_3$) δ 7.92 (s, 1H), 7.70 (d, *J* = 7.5 Hz, 2H), 7.59 (t, *J* = 7.3 Hz, 1H), 7.51 (t, *J* = 7.5 Hz, 2H), 3.59 (t, *J* = 4.9 Hz ,2H), 3.43 (t, *J* = 4.9 Hz, 2H), 3.00 (t, *J* = 4.7 Hz, 2H), 2.95 (t, *J* = 4.8 Hz, 2H). ^{13}C NMR (400 MHz, $CDCl_3$) δ 160.6, 135.2, 133.3, 129.2, 127.5, 46.5, 45.4, 44.8, 39.2. HRMS (ESI) calcd for $C_{11}H_{14}N_2O_3S$ $[M+H]^+$ m/z: 255.0788 found 255.0796.

2.2. Pharmacological/biological assay

α-Glucosidase inhibitory activity of samples obtained was measured according to the method also explained by Balan *et al*. [16]. Firstly, proper amounts of monosodium phosphate and disodium phosphate were mixed with procuring 100 mM phosphate buffer (pH 7). Then, α-glucosidase enzyme was dissolved in phosphate buffer to obtain α-glucosidase solution (0.2 U/mL). Later, 170 µL of phosphate buffer, 20 µL of

α-glucosidase solution and 20 µL of sample solutions were mixed and incubated in 37 °C oven for 15 min. After that, 20 µL of 2.5 mM p-nitrophenyl-α-D-glucopyranoside solution in 100 mM potassium phosphate buffer (pH 7.0) was added to the mixture, and another incubation period was executed at 37 °C for 15 min. Then, 80 µL of 0.2 M sodium carbonate solution was appended to the mixture to terminate the reaction. Absorbance was measured at 405 nm. Quercetin was used as a reference solution at 31.25, 62.5, 125, 250, 500 and 1000 µg/mL concentrations. Results were estimated as the percentage of inhibitory activity in 1 mg/mL concentrations of samples.

2.3. Molecular docking

Method details. Ligand Preparation: SDF files of ligands were generated using Data Warrier. Briefly, SMILES codes are used to generate conformers with setting as following: Random, Low Energy Bias, Torsions based on crystallographic database, energy minimization based on MMFF94s+ Forcefield. SD file version 3 with 3D atom coordinates has been used. Docking Parameters and Protein Preparation: PDB ID: 5NN5 Alpha-glucosidase (Homo sapiens) in complex with 1-deoxynojirimycin has been used to for docking studies. Briefly, crystal structure of protein was downloaded in pdb format from https://www.rcsb.org. PDB ID: 5NN5 structure was optimized for docking by removing of water molecules, 1-deoxynojirimycin, chloride ions, 1,2-ethanediols, sulfate ions and other chains (B-F). A grid box with 26Åx26Åx26Å and coordinates of x=-15.43, y=-37.864, z=93.588 and spacing of 1Å around the 1-deoxynojirimycin binding pocket (for PDB ID: 5NN5) has been generated using AutoDockTools 1.5.6. Automated docking of ligands was performed with PaDelADV. To investigate the interaction of molecules and enzymes' amino acids BIOVIA Discovery studio was used.

3. Results and Discussion

3.1. Chemistry

Compounds **1-5** were synthesized according to refence [13] with some modifications. Briefly, piperazine was dissolved in CH_2Cl_2 (DCM) derivatives (1.0 eq) and triethylamine (3.0 eq) was added to solution slowly at 0 °C. Then this mixture was added to benzene sulfonyl chloride (1.0 eq) and stirred for 2 hours at room temperature. The completion of the reaction was checked with TLC. After the reaction was finished, water was added, and extraction was done with DCM. The combined organic layer was dried over anhydrous Na_2SO_4 and evaporated to give compounds **1-5** (**Figure 1**). Compounds were characterized with ^{1}H-NMR, ^{13}C-NMR and HRMS. In ^{1}H-NMR spectrum, basic peaks of aromatic hydrogens of compounds were observed at 7.70 – 7.50 ppm. Aliphatic hydrogens of the piperazine ring were found 3.50 – 2.0 ppm. The peaks of these hydrogens were designated in two different manners. Some of them had only one peak and others had two peaks according to the substituent on piperazine ring.

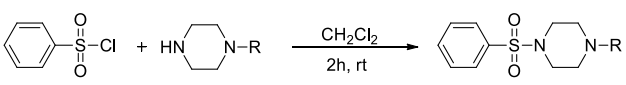

Figure 1. Synthesis pathway of compounds **1-5**

3.2. Enzyme inhibition

Five piperazine sulfonamide derivatives (**1-5**) were synthesized and investigated for α-glucosidase enzyme inhibition activity. Quercetin was used as a reference molecule, because of its well-known α-glucosidase inhibitory potential. According to the results of study, all compounds have good inhibitory activities (63.45 ± 0.14 – 83.52 ± 0.41) against α-glucosidase enzyme (**Table 1**). Compound **1** has higher inhibition values than quercetin and the most active compound against α-glucosidase enzyme in this series. The phenyl group that was attached to the piperazine which is substituted with EDG group like methoxy as in compound **4** showed the lowest inhibition value. This result cannot be only correlated with the EDG, but this can be explained by the different binding states of the substituents to the enzyme. Lastly, compound **5** has reasonable inhibition value. It can be resulted from EWG on the phenyl group. According to this result, different types of substituents have high α-glucosidase enzyme inhibition activity in this series.

3.3. Molecular docking

Molecular docking is an important tool for elucidating the structural properties of ligands that have biological activity for target enzymes. In this part, the most active compound was investigated based on their molecular interactions and binding energies for α-glucosidase enzymes. A molecular docking study was done for the most potent compound **1**. The binding energy of compound **1** was calculated and found to be -5.3 kcal/mol. For compound **1**, the phenyl group has two different types of interaction: π-anion interaction between ASP518 and π-π stacks with PHE649 and TRP376. Moreover, sulfonamide group has π-sulfur interaction with TRP481 and hydrogen bond formation between ARG600. In addition, carbon hydrogen bond interaction between ASP616 (**Figure 2**).

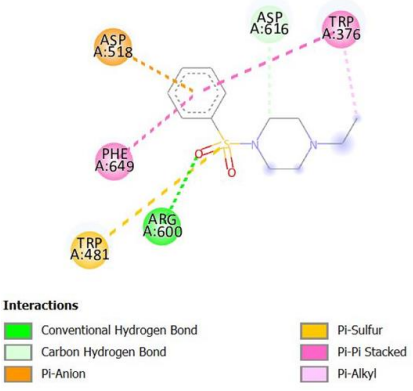

Figure 2. Docking result of the compound **1** for α-glucosidase enzyme

Table 1. α-Glucosidase enzyme inhibition results of compounds **1-5**

Compounds	R	α-Glucosidase enzyme inhibition (%)
1	$-CH_2CH_3$	82.48 ± 0.21
2		77.45 ± 0.13
3		75.68 ± 0.23
4	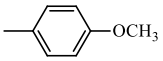	63.45 ± 0.14
5	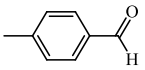	77.35 ± 0.45
Quercetin		81.41 ± 0.02

[a]Results were presented as α-glucosidase enzyme inhibition experiments were performed independently three different times. [b]Standard deviation was symbolized with ±.

3.4. ADME profiling

ADME (absorption, distribution, metabolism, and excretion) is an important factor for the development of biologically active oral drug candidates. ADME parameters of compounds were investigated using the freely accessible silico SwissADME web tool (http://www.swissadme.ch). This tool provides bioavailability radar and boiled-egg charts. Bioavailability radar charts contain physicochemical properties that are used to explore physicochemical characteristics and drug-likeness properties of molecules. The physicochemical properties of compounds **1-5** were predicted with SwissADME free web tool [17]. The bioavailability radar indicates rapid pre-assessment of drug-likeness. In this chart six main physicochemical properties are investigated, these are lipophilicity, polarity, size, solubility, saturation, and flexibility (**Figure 3**). The part within the pink area is the border drawn for the physicochemical properties of the molecules to be a drug-likeness. When the red frame of the molecules is in the pink area, it shows that the physicochemical values of the molecule remain within the desired limits. Calculated physicochemical properties of compounds (**1** – **5**) are in desired limits and in pink area. These charts indicate that lipophilicity, oral

bioavailability, and solubility of compounds are suitable for drug-likeness properties.

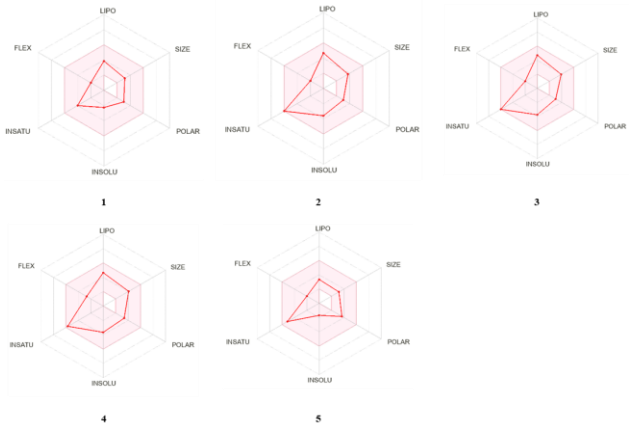

Figure 3. Bioavailability radar chart of compounds **1-5**

3.5. Quantum mechanical calculations

3.5.1. Computational DFT method

Density functional theory (DFT) with the Gaussian 09 were used to optimize geometry. At the B3LYP/6-31+G level of theory [18], [19] DFT approaches were utilized to refine the geometry of a promising molecule. The lowest unoccupied molecular orbital (LUMO), and highest occupied molecular orbital (HOMO) localization energies of promising molecules were investigated. Data from DFT analyses revealed that the five molecules were ordered by their chemical reactivity as follows: molecules **2**, **4**, **3**, **1**, and **5** respectively. The primary step in computing quantum chemicals for a molecular system is geometry optimization. Finding the conditions under which the molecule is most stable, or where the energy is lowest, is the aim of geometry optimization. The entire quantum chemical calculations have been performed at DFT (B3LYP) methods 6-31+G basis set using the Gaussian 09W software package [20]. **Table 2** displays both the geometrical parameters derived from optimized geometry data and the optimized molecular structure of molecules **1** - **5** as determined by DFT calculations at the B3LYP level using a 6-31+G basis set. The bond length, bond angles and torsional angles of optimized molecule **2** are shown in **Table 3**. Frontier molecular orbitals were employed to assess the electrical properties and electron transport potential of the compounds under investigation. These orbitals determine the molecular characteristics and biological activity of the substances. The LUMO, which represents the electron-deficient orbital, is associated with the ability to accept electron density and electron affinity. On the other hand, the HOMO, representing the electron-rich orbital, is proportional to the ionization potential.

Table 2. Gaussian-based calculations of frontier molecular orbital energies of molecules **1-5**

Compounds	HOMO (eV)	LUMO (eV)	Energy Gap- ΔE (eV)
1	-0.20843	-0.06621	0.14222
2	-0.20197	-0.07080	0.13117
3	-0.21012	-0.07827	0.13185
4	-0.19923	-0.06765	0.13158
5	-0.26323	-0.07662	0.18661

The energies of the LUMO and HOMO govern the molecule's interactions with other species and contribute to its chemical reactivity and kinetic stability. A small difference between the LUMO and HOMO energies indicates a low band energy gap (ΔE), suggesting a compound's higher reactivity with a receptor. A smaller energy gap signifies greater reactivity since the LUMO and HOMO are responsible for charge exchange during chemical reactions [21], [22]. The reactivity order among the ten molecules was found to be **2** > **4** > **3** >**1** > **5**, with compound molecule **2** exhibiting the smallest band energy gap, indicating its highest reactivity compared to the others. In molecule **2**, the HOMO is localized on the piperazine moiety, while the LUMOs are localized on the benzenesulfonyl and some portion of the piperazine scaffold. The highly delocalized HOMO suggests that electrons can move more freely within the molecule, leading to improved intramolecular charge transfer (**Figure 4**).

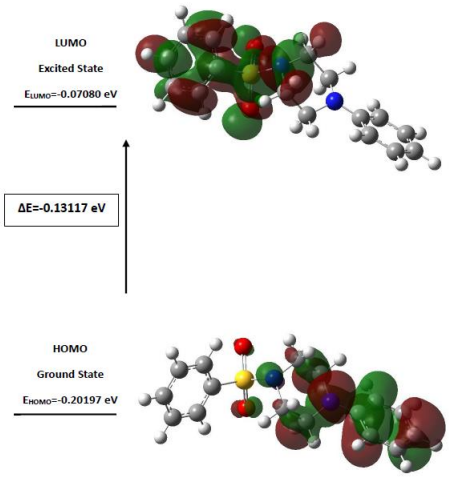

Figure 4. HOMO, LUMO energy of the compound molecule **2**.

Table 3. B3LYP/6-31+G level of basis set's computed optimum geometrical parameters for molecule **2**.

Bond lengths (Å)		Bond angle (°)			Torsional angle (°)		
C1-C2: 1.40062	C25-C27: 1.41473	C6-C1-C2: 120.12889	H39-C16-N23: 104.76470	C26-C28-C32: 120.87460	C1-C2-C3-C4: 0.62773	O14-S12-N23-C16: -36.50082	N24-C25-C27-H31: -0.69937
C1-C6: 1.40363	C26-C28: 1.40110	H7-C1-C6: 120.25198	H39-C16-C19: 109.84204	H33-C28-C26: 119.05799	C1-C2-C3-S12: 178.79721	C15-C17-N24-C19: -58.35667	N24-C25-C26-C28: 177.94183
C1-H7: 1.08498	C26-H29: 1.08347	H7-C1-C2: 119.61849	C15-C17-N24: 110.25336	H33-C28-C32: 120.06155	C1-C6-C5-H10: 179.42996	C15-N23-C16-C19: 45.03652	N24-C25-C27-C30: -178.58698
C2-C3: 1.39215	C27-C30: 1.39630	C1-C2-C3: 117.80224	H21-C17-H37: 107.98579	C27-C30-C32: 120.77630	C2-C3-C4-C5: 0.62267	C15-C17-N24-C25: 154.02944	C25-C26-C28-C32: 0.73283
C2-H8: 1.08381	C27-H31: 1.08484	H8-C2-C1: 121.49330	H21-C17-C15: 109.48725	H34-C30-C32: 119.99845	C2-C3-C4-H9: 178.43062	C15-N23-C16-H20: 169.13079	C25-C27-C30-C32: 0.51527
C3-C4: 1.39109	C28-C32: 1.39897	H8-C2-C3: 120.70311	H21-C17-N24: 110.33388	H34-C30-C27: 119.21736	C2-C3-S12-O13: -174.53970	C15-N23-C16-H39: -75.32334	C25-C26-C28-H33: 179.85327
C3-S12: 1.87148	C28-H33: 1.08629	C2-C3-C4: 123.66214	H37-C17-C15: 109.06070	C28-C32-C30: 118.79517	C2-C3-S12-O14: -43.39410	C16-C19-N24-C17: 57.57380	C25-C27-C30-H34: 179.56022
C4-C5:1.40289	C30-C32: 1.40317	S12-C3-C2: 118.42090	H37-C17-N24: 109.67615	H35-C32-C30: 120.55976	C2-C1-C6-H11: 179.82806	C16-N23-C15-C17: -45.44815	C26-C28-C32-C30: -0.27875
C4-H9:1.08457	C30-C34: 1.08630	S12-C3-C4: 117.89274	C16-C19-N24: 110.18807	H35-C32-C28: 120.64507	C3-C4-C5-C6: 0.17980	C16-N23-C15-H18: 74.97009	C26-C25-C27-C30: -0.06606
C5-C6:1.40155	C32-C35: 1.08513	C3-C4-C5: 117.79537	H22-C19-H38: 107.91906		C3-C4-C5-H10: 179.83731	C16-N23-C15-H36: -169.68266	C26-C25-N24-C19: -11.33074
C5-H10:1.08501		H9-C4-C3: 120.03339	H22-C19-C16: 107.97814		C3-S12-N23-C15: 79.97705	C16-N23-S12-O13: 96.17470	C26-C25-N24-C17: 133.94363
C6-H11:1.08537		H9-C4-C5: 122.16416	H22-C19-N24: 109.07734		C3-S12-N23-C16: -150.50221	C16-C19-N24-C25: -154.99164	C26-C25-C27-H31: 177.82155
S12-O13:1.50103		C4-C5-C6: 120.10095	H38-C19-C16: 109.90970		C4-C5-C6-C1: 0.22496	C17-N24-C19-H22: 175.94165	C26-C28-C32-H35: 179.71158
S12-O14:1.50103		H10-C5-C6: 120.32319	H38-C19-N24: 111.66519		C4-C5-C6-H11: 179.83293	C17-N24-C19-H38: -64.87002	C27-C25-C26-C28: -0.55045
C15-C17: 1.53349		H10-C5-C4: 119.57497	C15-N23-C16: 113.50443		C4-C3-C2-H8: 178.95736	C19-N24-C17-H21: 62.70456	C27-C30-C32-C28: -0.34113
C15-H18: 1.09793		C1-C6-C5: 120.50718	S12-N23-C16: 112.08208		C4-C3-S12-O13: 3.73648	C19-N24-C17-H37: -178.46389	C27-C25-N24-C17: -47.59573
C15-N23: 1.48684		H11-C6-C5: 119.77744	S12-N23-C15: 112.71052		C4-C3-S12-O14: 134.88208	N23-C16-C19-N24: -178.46389	C27-C25-N24-C19: 167.12989
C15-H36: 1.09436		H11-C6-C1: 119.71422	C17-N24-C19: 112.47201		C5-C6-C1-C2: 0.21984	N23-C15-C17-N24: 51.51380	C27-C25-C26-H29: 178.08067
C16-C19:1.53564		O13-S12-O14: 119.72057	C25-N24-C17: 119.17263		C5-C6-C1-H7: 179.49073	N23-C15-C17-H21: -70.05152	C27-C30-C32-H35: 179.66853
C16-N23:1.48464		C17-C15-N23: 113.76871	C25-N24-C19: 119.67221		C5-C4-C3-S12: 178.80115	N23-C15-C17-H37: 171.99138	C28-C32-C30-H34: -179.37864
C16-H20:1.09324		H18-C15-C17: 110.10835	C26-C25-C27: 117.95607		C6-C1-C2-C3: 0.18978	N23-C16-C19-H22: -169.57294	C30-C32-C28-H33: -179.39041
C16-H39:1.09762		H18-C15-N23: 104.93945	N24-C25-C26: 121.92734		C6-C1-C2-H8: 179.39184	N23-C16-C19-H38: 72.93938	C32-C30-C27-H31: -177.38460
C17-H21: 1.10206		H18-C15-H36: 107.86922	N24-C25-C27: 120.09940		S12-N23-C15-C17: 178.80115	N23-S12-C3-C2: 72.93938	
C17-N24: 1.47933		H36-C15-N23: 109.04865	C25-C26-C28: 120.71204		S12-N23-C15-H18: -156.24326	N23-S12-C3-C4: -115.26063	
C19-H22: 1.09351		H36-C15-C17: 110.80128	C25-C27-C30: 120.88104		S12-N23-C16-H20: 40.02372	N24-C17-C15-H18: -65.95160	

4. Conclusion and Suggestions

In this study, five phenylsulfonyl piperazine derivatives were synthesized. Their inhibitory potentials against α-glucosidase enzyme were evaluated. Compound **1** has a higher inhibition value than the reference molecule quercetin in the α-glucosidase enzyme assay. The other molecules had valuable α-glucosidase enzyme inhibition values. Bioavailability radar chart was used to study the physicochemical properties and compliance with the Lipinski rule of five molecules. Acceptable drug-like and pharmacokinetic properties were expected from the synthesized molecules according to the results. In addition, docking studies and DFT calculations have been carried out. Molecular docking studies were performed to identify the significant interactions between molecules and enzymes. These promising results were confirmed by their binding energy of compound **1** was -5.3 kcal/mol for the α-glucosidase enzyme. The enzyme inhibition results were in good agreement with the docking studies. Although, DFT calculations showed that compound **2** had the lowest energy gap (ΔE (eV): 0.13117), that may be the most active compound, but it was the second the most potent α-glucosidase enzyme inhibitor. Consequently, all these results suggest these molecules, especially compound **1**, as potential leads for further optimization of antidiabetic molecules.

Acknowledgment

This project was supported by the University of Health Sciences, unit of scientific research project (BAP) (Project No:2020/040). The Gaussian calculations made in the article were made in the Marmara University Computational Chemistry Laboratory. We would like to thank Safiye Sağ Erdem for her support.

Contributions of the authors

Plan and design of the study: KB; Data collection: Yİ, GSA, CDÖ; Data analysis and interpretation: KB, CDÖ, FK; Writing-critical evaluation: KB, FK.

Conflict of Interest Statement

There is no conflict of interest between the authors.

Statement of Research and Publication Ethics

The study is complied with research and publication ethics.

References

[1] M. J. Fowler, "Microvascular and Macrovascular Complications of Diabetes," *Clinical Diabetes*, vol. 26, no. 2, pp. 77–82, Apr. 2008.

[2] M. Dehghan *et al.*, "Progress toward molecular therapy for diabetes mellitus: A focus on targeting inflammatory factors," *Diabetes Res Clin Pract*, vol. 189, p. 109945, Jul. 2022.

[3] A. S. Alqahtani *et al.*, "Alpha-amylase and alpha-glucosidase enzyme inhibition and antioxidant potential of 3-oxolupenal and katononic acid isolated from Nuxia oppositifolia," *Biomolecules*, vol. 10, no. 1, 2020.

[4] M. D. P. T. Gunawan-Puteri, E. Kato, and J. Kawabata, "α-Amylase inhibitors from an Indonesian medicinal herb, Phyllanthus urinaria," *J Sci Food Agric*, vol. 92, no. 3, pp. 606–609, Feb. 2012.

[5] E. Vitaku, D. T. Smith, and J. T. Njardarson, "Analysis of the Structural Diversity, Substitution Patterns, and Frequency of Nitrogen Heterocycles among U.S. FDA Approved Pharmaceuticals," *J Med Chem*, vol. 57, no. 24, pp. 10257–10274, Dec. 2014.

[6] M. K. Akkoç, M. Y. Yüksel, I. Durmaz, and R. E. Atalay, "Design, synthesis, and biological evaluation of indole-based 1,4-disubstituted piperazines as cytotoxic agents," *Turk J Chem*, vol. 36, no. 4, pp. 515–525, 2012.

[7] D. Mukherjee, A. Mukhopadhyay, K. S. Bhat, A. M. Shridhara, and K. S. Rao, "Synthesis, characterization and anticonvulsant activity of substituted 4- chloro-2-(4-piperazin-1-YL) quinazolines," *Int J Pharm Pharm Sci*, vol. 6, no. 5, pp. 567–571, 2014.

[8] T. Kálai, M. Khan, M. Balog, V. K. Kutala, P. Kuppusamy, and K. Hideg, "Structure-activity studies on the protection of Trimetazidine derivatives modified with nitroxides and their precursors from myocardial ischemia-reperfusion injury," *Bioorg Med Chem*, vol. 14, no. 16, pp. 5510–5516, 2006.

[9] K. Buran, R. Reis, H. Sipahi, and F. E. Önen Bayram, "Piperazine and piperidine-substituted 7-hydroxy coumarins for the development of anti-inflammatory agents," *Arch Pharm (Weinheim)*, vol. 354, no. 7, p. e2000354, 2021.

[10] K. Buran, S. Bua, G. Poli, F. E. Ö. Bayram, T. Tuccinardi, and C. T. Supuran, "Novel 8-substituted coumarins that selectively inhibit human carbonic anhydrase IX and XII," *Int J Mol Sci*, vol. 20, no. 5, 2019.

[11] A. Ignat, V. Zaharia, C. Mogoşan, N. Palibroda, C. Cristea, and L. Silaghi-Dumitrescu, "Heterocycles 25. Microwave assisted synthesis of some p-toluensulfonyl- hydrazinothiazoles with analgesic and anti-inflammatory activity," *Farmacia*, vol. 58, no. 3, pp. 290–302, 2010.

[12] R. A. Finch, K. Shyam, P. G. Penketh, and A. C. Sartorelli, "1,2-Bis(methylsulfonyl)-1-(2-chloroethyl)-2-(methylamino)carbonylhydrazine (101M): A novel sulfonylhydrazine prodrug with bbroad-spectrum antineoplastic activity," *Cancer Res*, vol. 61, no. 7, pp. 3033–3038, 2001.

[13] M. Taha *et al.*, "Synthesis of piperazine sulfonamide analogs as diabetic-II inhibitors and their molecular docking study," *Eur J Med Chem*, vol. 141, pp. 530–537, 2017.

[14] J. L. Xiao, R. S. Luo, Y. Shi, Q. Guo, Z. X. Zhou, and C. S. Zhao, "Synthesis, crystal structure and dft study of benzenesulfonamide compounds 1-ethyl-4-(phenylsulfonyl)piperazine and 1-((3-bromophenyi)sulfonyl)-4-methyipiperazine," *Molecular Crystals and Liquid Crystals*, vol. 755, no. 1, pp. 80–90, 2023.

[15] M. A. Abbasi *et al.*, "Synthesis, enzyme inhibition and molecular docking studies of 1- arylsulfonyl-4-Phenylpiperazine derivatives," *Pak J Pharm Sci*, vol. 30, no. 5, pp. 1715–1724, 2017.

[16] K. Balan, P. Ratha, G. Prakash, P. Viswanathamurthi, S. Adisakwattana, and T. Palvannan, "Evaluation of invitro α-amylase and α-glucosidase inhibitory potential of N2O2 schiff base Zn complex," *Arabian Journal of Chemistry*, vol. 10, no. 5, pp. 732–738, 2017.

[17] A. Daina, O. Michielin, and V. Zoete, "SwissADME: A free web tool to evaluate pharmacokinetics, drug-likeness and medicinal chemistry friendliness of small molecules," *Sci Rep*, vol. 7, no. October 2016, pp. 1–13, 2017.

[18] C. W. Bauschlicher Jr. and H. Partridge, "A modification of the Gaussian-2 approach using density functional theory," *J Chem Phys*, vol. 103, no. 5, pp. 1788–1791, Aug. 1995.

[19] A. M. Toth, M. D. Liptak, D. L. Phillips, and G. C. Shields, "Accurate relative pKa calculations for carboxylic acids using complete basis set and Gaussian-n models combined with continuum solvation methods," *J Chem Phys*, vol. 114, no. 10, pp. 4595–4606, Mar. 2001.

[20] M. J. Frisch *et al.*, "Gaussian 09, Revision A.02." Gaussian, Inc., Wallingford CT, 2016.

[21] M. Govindarajan and M. Karabacak, "Spectroscopic properties, NLO, HOMO–LUMO and NBO analysis of 2,5-Lutidine," *Spectrochim Acta A Mol Biomol Spectrosc*, vol. 96, pp. 421–435, Oct. 2012.

[22] M. A. Mumit, T. K. Pal, M. A. Alam, M. A. A. A. A. Islam, S. Paul, and M. C. Sheikh, "DFT studies on vibrational and electronic spectra, HOMO–LUMO, MEP, HOMA, NBO and molecular docking analysis of benzyl-3-N-(2,4,5-trimethoxyphenylmethylene)hydrazinecarbodithioate," *J Mol Struct*, vol. 1220, p. 128715, Nov. 2020.